JOURNAL OF MATERIALS SCIENCE **35** (2000) 4275–4288

Aluminium-27 solid state NMR spectroscopic studies of chloride binding in Portland cement and blends

J. A. CHUDEK, G. HUNTER*, M. R. JONES‡, S. N. SCRIMGEOUR
Departments of Chemistry and ‡Civil Engineering, University of Dundee, Dundee DD1 4HN, UK

P. C. HEWLETT
British Board of Agrément, PO Box 195, Bucknalls Lane, Watford, Herts WD2 7NG, UK

A. B. KUDRYAVTSEV
Analytical Centre, D. Mendeléev University of Chemical Technology of Russia, Miusskaya Sq. 9, 125190 Moscow, Russian Federation
E-mail: g.hunter@dundee.ac.uk

Alumina-rich pozzolanic and latent hydraulic binders such as pulverised fuel ash, metakaolin, and ground granulated blast furnace slag, together with silica fume, are frequently added to Portland cement concrete to improve performance and to retard chloride ingress and thereby inhibit chloride-induced corrosion of the carbon steel reinforcement. $^{27}Al\{^{1}H\}$ MAS and CP/MAS NMR spectroscopies have been used to follow both the hydration processes of the cement blends and the interactions of chloride ion with the hydrated aluminium species. The spectra of the hydrated aluminate phases were interpretable on the basis that the AFt (Aluminate Ferrite tri-) phase ettringite, $C_6A\bar{S}_3H_{32}$[§] ($3CaO{\cdot}Al_2O_3{\cdot}3CaSO_4{\cdot}32H_2O$, or $C_3A{\cdot}3CaSO_4{\cdot}32H_2O$), and the AFm (Aluminate Ferrite mono-) phases calcium mono-sulphoaluminate, $C_4A\bar{S}H_{12}$ ($3CaO{\cdot}Al_2O_3{\cdot}CaSO_4{\cdot}12H_2O$, or $C_3A{\cdot}CaSO_4{\cdot}12H_2O$), and the lamellar tetracalcium aluminate hydrate, C_4AH_{13} ($3CaO{\cdot}Al_2O_3{\cdot}Ca(OH)_2{\cdot}12H_2O$, or $C_3A{\cdot}Ca(OH)_2{\cdot}xH_2O$) were present as the only hydrated species containing octahedrally-coordinated aluminium. In all cases, only the AFm phase Friedel's salt ($3CaO{\cdot}Al_2O_3{\cdot}CaCl_2{\cdot}10H_2O$, or $C_3A{\cdot}CaCl_2{\cdot}10H_2O$) could be identified as the major chloroaluminate phase produced by the interactions of the cement pastes with chloride ion.

The unsightly rust stains, cracks, spalls and patchwork repairs that disfigure many concrete structures are all too familiar. These mostly result from the *carbonation* of the concrete by atmospheric carbon dioxide, causing corrosion and consequent disruptive expansion of the steel reinforcement. However, more serious consequences can result from corrosion of the reinforcement caused by the ingress of *chloride* ion. The demand for ice-free roads has meant that Britain, in common with many other countries with a temperate climate, necessarily applies large quantities of de-icing salts to highways. Other structures, particularly estuarine bridges, are also subject to marine salt and here the problem is compounded by year round contact with chloride rather than just in the winter months.

The ubiquity of Portland cement (***pc***) concrete in construction results from its ease of production on demand, its low cost, and the inherent chemical robustness of the calcium silicate hydrates that dominate its microstructure. Steel and concrete are chemically very well matched as the hydroxides of calcium, sodium, and potassium produced by the hydration of Portland cement result in its capillary pore fluids being highly alkaline, with a typical pH of between 12.5 and 13.5. This produces a 'passive' layer on embedded plain carbon steel reinforcement and if this remains undisturbed then corrosion will not occur and the structure remains durable and serviceable almost indefinitely. However, even very low concentrations of chloride reaching the surface of the reinforcement can cause destructive corrosion of the reinforcement [1].

Engineers have long searched for reliable but simple and cost effective solutions to the problem of chloride-induced corrosion. Fortunately, *aluminate phases* occur in both Portland cement and other latent hydraulic binders and, particularly, in many silico-aluminate

*Author to whom all correspondence should be addressed.
§Note the cement chemists' shorthand notation: $A = Al_2O_3$; $C = CaO$; $F = Fe_2O_3$; $H = H_2O$; $S = SiO_2$; $\bar{S} = SO_3$.

pozzolanic binders, and are capable of reacting and combining with chloride ions. Pozzolanas are siliceous or siliceous and aluminous materials, which in themselves possess little or no cementitious value but which, in finely divided form and in the presence of moisture, chemically react with calcium hydroxide to form calcium silicate and calcium aluminate compounds, similar to those which are formed from the hydration of Portland cement [2]. Latent hydraulic binders and pozzolanas used in structural concrete are: ground granulated blastfurnace slag (***ggbs***), made by the rapid cooling of a blast furnace slag melt with a composition at least two thirds by mass of the sum of CaO, MgO, and SiO_2 and with the ratio by mass $(CaO + MgO) : SiO_2 \geq 1$. The remainder contains Al_2O_3 (5–17%) [3a]; pulverised fuel ash (***pfa***), obtained by electrostatic or mechanical precipitation of dust-like silico-aluminous particles from the flue gases from furnaces fired by pulverised bituminous coal, Al_2O_3 content range 28–35% [3b,c]; burnt shale (***bs***) - specifically burnt oil shale, produced in a kiln at 800°C whose clinker phases contain mainly dicalcium silicate and monocalcium aluminate. Calcium oxide content 16–60% [3b]; silica fume (***sf***), from the reduction of high purity quartz with coal in an electric arc furnace in the production of silicon and ferrosilicon alloys, which consists of very fine spherical particles with a high content of amorphous silica [3d]; thermally-activated *meta*-kaolin (***mk***) which is a pink or white powder produced by calcining kaolinitic clay at 750°C. It is mainly amorphous alumino-silicate, consisting of silica (∼51%) and alumina (∼42%), but with only a very small amount (<1%) of calcium oxide and therefore on its own does not have hydraulic properties [3e].

By using combinations of these binders, the concentration of aluminates can be increased and hence potentially provide an enhanced capacity for chloride binding as well as refining the capillary pore structure of the concrete and physically inhibiting the chloride flux [4].

1. ^{27}Al NMR Spectroscopy

^{27}Aluminium (100% abundant, $I = 5/2$) is a half-integral quadrupolar nucleus and, as such, the interpretation of its high resolution MAS and CP/MAS solid state NMR spectra presents complications compared with those of dipolar nuclei. Nevertheless, this nuclide is of high sensitivity, naturally relaxes quickly, and its spectra can provide clues as to the chemical reactions of compounds of this element, crucial to an understanding of chloride binding in Portland Cement and its blends with Pozzolanic binders.

The solid state NMR spectra of quadrupolar nuclei are usually dominated by the quadrupolar term arising from the interaction of the non-spherically-symmetrical nuclear charge with an electrostatic field generated by the surrounding electrons. The product of the principal component of the field gradient and the quadrupolar moment eQ describes the quadrupolar coupling constant C_Q. Dipolar interactions, chemical shift anisotropy, and spin-spin couplings are normally small by comparison. Fortunately, for half-integral quadrupolar nuclei the central transition ($m_I = +1/2 \leftrightarrow m_I = -1/2$) is least affected by first-order quadrupolar effects, which for ^{27}Al can usually be averaged by Magic Angle Spinning (MAS) [5]. When the quadrupolar interaction is small ($C_Q \ll \omega_r$), no spinning side bands are observed, although their complete removal may require very fast rotation of up to 20 kHz [6].

However, anisotropic second order quadrupolar interactions are not fully removed by MAS and can be substantial, leading to residual asymmetry and line broadening of the ^{27}Al signal. For ^{27}Al five singularities (only three when the anisotropy factor η is 0.0 or 1.0) may be observed in the central transition of its MAS NMR spectrum [7]. The second order quadrupolar effect parameter, $SOQE = C_Q(1 + \eta^2/3)^{1/2}$, governs the degree of the second-order quadrupolar line broadening and line shifts at a particular magnetic field [8]. Moreover, the intensity and shape of the observed signal are also dependent on the power and flip angle of the exciting r.f. pulse [9]. In particular, when ^{27}Al nuclei occupy sites which experience different electric field gradients the spectra are quantitatively reliable only if the central transitions are selectively excited by a strong but short ($\leq \pi/2(2I + 1)$, i.e. $\pi/12$) rf. pulse [10]. For non-selective excitation, the maximum FID signal is measured after a $\pi/2$ pulse when the maximum intensity for the central transition is $4I(I + 1)/3(I + 1/2)$, i.e. 3.89, times greater than that obtained by selective excitation [9, 10a].

Chemical shift is directly proportional to B_0 whereas the second order quadrupolar interaction is inversely proportional to B_0, and the barycentre or centre of gravity, ν_{cg}, of the central transition is shifted by the quadrupolar interaction. There is therefore advantage in obtaining spectra at the highest possible spectrometer frequency when the quadrupolar interaction is minimised. Many ^{27}Al chemical shifts reported for solid samples are not the true isotropic chemical shifts, ν_{iso}, but rather represent the centres of gravity, ν_{cg}, of lines that contain considerable quadrupolar contributions [9]. The residual quadrupolar shift for the central transitions has been calculated [11] as,

$$(\nu_{iso} - \nu_{cg}) = 0.2667(\nu_Q/\nu_0)^{1/2}10^6$$

where ν_0 and ν_Q are, respectively, the Larmor and quadrupolar frequencies, with the latter given by,

$$\nu_Q = \frac{3\,C_Q(1 + \eta^2/3)^{1/2}}{2I(I + 1)}$$

When C_Q is small the shift of the central band approximates to

$$(\nu_{iso} - \nu_{cg}) = 0.8493\ \nu_{1/2}$$

where, $\nu_{1/2}$ is the line width at half height of the observed signal which is assumed to have a Gaussian shape [12], an assumption which, of course, becomes less valid with increasing C_Q.

Both first and second order effects can be eliminated in a single experiment by rapidly spinning the sample simultaneously about two angles to B_0. This is achieved in Double Oriented Rotation (DOR) spectroscopy where the sample is contained in an inner

rotor which rotates at high speed about an axis inclined at 30.6° to the axis of an outer rotor which is itself spun at a slower rate at the normal Magic Angle of 54.7° to B_0 [13]. However, like others [14], we have found that in the absence of ^{1}H decoupling to remove strong dipolar interactions, DOR gives *broader, less well-resolved*, spectra than simple MAS. This is probably because the maximum MAS frequency available for removing dipolar and first order quadrupolar interactions is that of the slower outer rotor. Second order quadrupolar interactions are, however, efficiently removed by the more rapidly rotating inner rotor [6].

No line narrowing technique can, of course, reduce line-broadening effects due to either the amorphous character of a sample or the presence of paramagnetic centres, such as Fe^{3+}, close to the observed nucleus. Cross Polarisation (CP) is normally used in solid state NMR spectroscopy to compensate for the long T_1's of dipolar nuclei and allow shorter recycle delays between scans, giving much shorter spectral acquisition times. Quadrupolar nuclei naturally relax more quickly and spectral acquisition over a realistic timescale does not normally require the application of CP, provided that the mechanical stresses induced by rapid magic angle spinning do not cause unacceptable physical or chemical changes to the sample, otherwise a very rapid spectral acquisition is necessary to minimise these effects (see below). Moreover, this technique transfers magnetisation from ^{1}H to ^{27}Al, which only occurs efficiently when the nuclei are spatially close, and CP/MAS spectroscopy potentially can provide valuable information about which part of the ^{27}Al signal arises from the hydrated part of the specimen. CP/MAS spectroscopy is more complicated for half-integral quadrupolar nuclei than it is for dipolar nuclei. The effects of both non-selective and selective CP on the shape of the ^{27}Al signal of *tris*-(2,4-pentandionato)aluminium(III), (Al(*acac*)$_3$), have been described [15]. Also, as MAS reduces both the size of the CP signal and the optimum contact time, to maintain signal strength, spinning should be as slow as possible as even at 2 kHz these effects may be noticeable [16].

2. Experimental

Commercial Portland cement was used to prepare all the cement paste samples. ***Pc*** and its mixes with other binders (pulverised fuel ash ***pfa***; ground granulated blastfurnace slag ***ggbs***; *meta*-kaolin ***mk***; burnt shale ***bs***; silica fume ***sf***) as well as a reference mix with the non-pozzolana powdered limestone ***ls*** were made up to the following ratios: 1.0 ***pc***; (*A* wt %, 5.1) : 0.70 ***pc***/0.30 ***pfa***; (12.8) : 0.50 ***pc***/0.50 ***ggbs***; (8.2) : 0.85 ***pc***/0.15 ***mk***; (10.4) : 0.50 ***pc***/0.50 ***bs***; (14.4) : 0.9 ***pc***/0.10 ***sf***; (4.6) : 0.9 ***pc***/0.10 ***ls***; (4.6). The oxide contents of the components of the dry binder samples are recorded in Table I. A water : solids ratio (conventionally, w/c) of 0.4 was used and the samples were mixed in a high shear blender, cast in refrigerator ice cube trays, and cured under water at 20°C for up to 6 months. Specimens for spectroscopy were removed at intervals, broken up, ground, and sieved (150 μm). The hydration process was followed for one year. Starting at six months after initial hydration, cement cubes were soaked in 5M NaCl solution for up to 6 months, when specimens were prepared for spectroscopy.

Tetracalcium aluminate hydrate: C_4AH_{13} was prepared according to the method of Skibsted *et al.* [8]. An excess (30%) of saturated calcium hydroxide solution was added to a solution of 1.0 g of sodium aluminate (Merck) dissolved in 50 ml of deionised water at room temperature. An immediate precipitate formed and the reaction mixture was left in a refrigerator overnight. The precipitate was filtered off, washed with acetone/water and then dried overnight in a desiccator over silica gel. It should be noted that the phase C_4AH_{13} is *meta*-stable and readily undergoes changes in water contents to form other AFm hydrates with higher/lower water molecule contents in the principal layer [17] and therefore unless specifically identified all the hydrates are referred to below as C_4AH_x. Both the ^{27}Al MAS and CP/MAS spectra showed a signal at the expected chemical shift and of the appropriate line width [8].

Friedel's salt: $C_3A{\cdot}CaCl_2{\cdot}10H_2O$ was prepared as described by Roberts [18]. 250 ml of a mixed $CaCl_2/AlCl_3$ solution containing 1.52 g of Al_2O_3 was added to 750 ml of a CO_2-free NaOH solution according to the equation

$$\begin{aligned} 5CaCl_2 + 2AlCl_3 + 14NaOH + 4H_2O \\ = 3CaO{\cdot}Al_2O_3{\cdot}CaCl_2{\cdot}10H_2O \\ + Ca(OH)_2 + 14NaCl \end{aligned}$$

and with an excess of NaOH calculated to give 0.01M NaOH solution on completion of the reaction. The mixture was shaken for seven days at 25°C. After filtering in CO_2-free air, the precipitate was washed with ethanol and diethyl ether and then dried at room temperature. Both the ^{27}Al MAS and CP/MAS spectra showed a single signal with some asymmetry (Fig. 1) which was readily deconvoluted into two quite narrow

TABLE I Oxide contents of the dry binders

Binder	Specific surface area ($m^2\ kg^{-1}$)	CaO (% wt)	SiO_2 (% wt)	Al_2O_3 (% wt)	Fe_2O_3 (% wt)	MgO (% wt)	TiO_2 (% wt)	Na_2O (% wt)	K_2O (% wt)	SO_3 (% wt)
pc	375	65.2	19.6	5.1	3.1	1.1	0.3	0.1	0.6	3.0
ggbs	380	39.6	36.6	11.3	0.9	8.2	0.5	0.4	0.6	0.3
pfa	450	2.2	49.6	30.9	9.7	1.3	1.0	0.9	4.0	0.9
mk	—	0.0	55.1	40.4	0.6	0.4	0.0	0.0	0.0	0.0
sf	23,000	0.3	98.0	0.1	0.2	0.9	0.0	0.4	0.7	0.0
bs	1,590	2.3	56.1	23.6	8.2	1.9	1.2	0.5	2.3	0.3

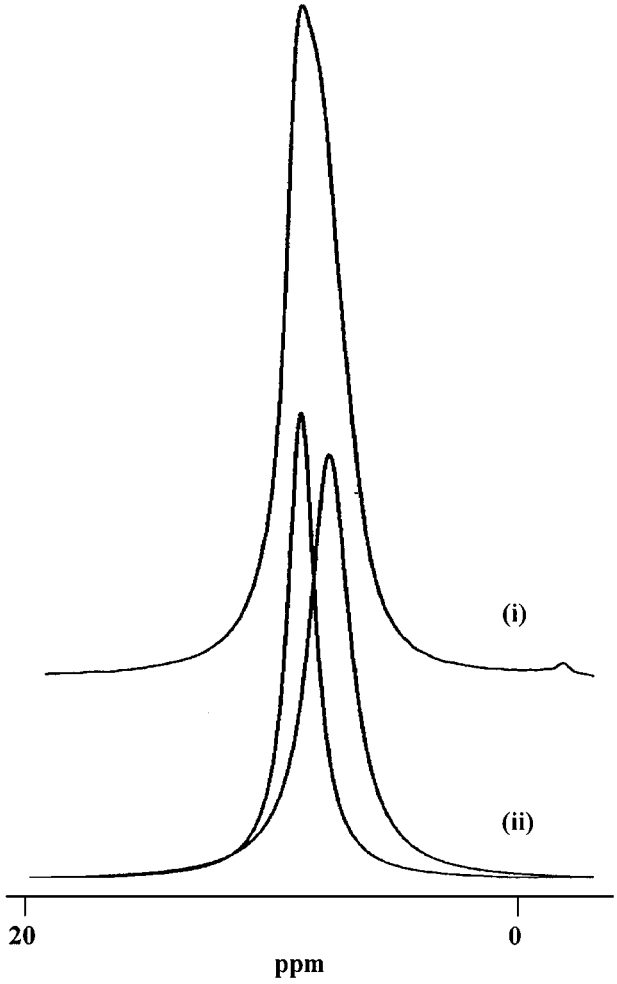

Figure 1 78.17 MHz ^{27}Al-{^{1}H} *pda* MAS solid state NMR spectrum of Friedel's salt ($C_3A{\cdot}CaCl_2{\cdot}10H_2O$); (i) observed; (ii) deconvoluted.

Gaussian-shaped lines of similar integral (ν_{cg}, 7.9, 9.1 ppm; $\nu_{1/2}$, 187, 149 Hz (2.4, 1.9 ppm respectively)) .

2.1. NMR Spectroscopy

^{27}Al solid state NMR spectra were recorded using a Chemagnetics CMX-300 Lite NMR spectrometer (^{1}H, 300.07 MHz; ^{27}Al, 78.17 MHz). Stresses induced by the large centrifugal forces associated with magic angle spinning caused longitudinal fractures in samples *cast* in the rotors. Samples were therefore powdered, sieved (150 μm) and spun at the magic angle in 7.5 mm o.d. zirconia Pencil® rotors. The spinning rate (4.2 kHz), and the power and length of the exciting r.f. pulse were carefully controlled. Unless otherwise recorded in the text, all data were accumulated within the first hour of spinning time (see below). All time domain data were transformed into 2048 word spectra using 5 Hz line broadening. High power ^{1}H decoupling caused significant line narrowing of the signals arising from six-, but not four-, co-ordinated aluminium contained in the hydrated cement pastes. Therefore in the hydrated aluminium species, dipolar and/or scalar interactions were sufficiently large not to have been completely removed by MAS alone. High power ^{1}H decoupling was achieved during the acquisition period in both the MAS (one pulse spectra, *pda*) and CP/MAS experiments, using the ^{1}H and ^{27}Al power levels determined for the CP experiments (^{27}Al 90° pulse width, 4 μs; acquisition time, 1.021 s; sweep width, 100 kHz; time domain data size, 2048 words; maximum number of acquisitions, 2000). The acquisition cycle repetition rate was sufficiently slow to exclude any significant heating of the sample.

Tris-(2,4-pentandionato)aluminium(III), Al(*acac*)$_3$, (Aldrich Chemical Co. Ltd.) was added to the samples as a secondary standard, itself being referenced to 1 M $AlCl_3$ solution. Al(*acac*)$_3$ has the quadrupolar coupling constant $C_Q = 3.0$ MHz and asymmetry factor $\eta = 0.15$ and an unusually well-defined quadrupolar line shape [15]. While the value for the isotropic chemical shift (ν_{iso}) for Al(*acac*)$_3$ is 0.0 ppm, the five singularities observed in the central transition of its MAS NMR spectrum all occur just upfield of the range of the resonances of the octahedral aluminium environments of the cement mixtures, making it an excellent secondary chemical shift standard for this work. Moreover, as the shape of its signal is sharply dependent on the experimental conditions, it also acted as a monitor for r.f. power and flip angle.

Fig. 2 shows the ^{27}Al-{^{1}H} spectrum of hydrated Portland cement with added Al(*acac*)$_3$ obtained with a constant ^{27}Al power level $\omega_{rf} \approx 62$ kHz, but with the rf pulse length t_p varying from 0.5 to 5.5 μs, corresponding to flip angles from 11° to 110°. As anticipated, the length of the r.f. pulse had an effect on the intensities of the signals and their line shapes [9, 10a], particularly that of the Al(*acac*)$_3$ secondary standard. The cement resonance at ν_{cg}, 13.2 ppm (assigned to ettringite; see below) reached its maximum intensity at $t_p = 4.0$ μs, whereas that at higher field (assigned to mono-aluminosulphate) had peaked at 3.0 μs, this behaviour being consistent with the significantly larger quadrupolar coupling constant of the latter species [10a] (ettringite C_Q, 0.36; mono-sulphoaluminate C_Q, 1.7 MHz [8]).

Cross-polarisation experimental conditions were established using a sample of pure kaolin [19]. The transmitter power levels were set to give a true Hartmann-Hahn matching condition:

$$\gamma_{(Al)} B_{1(Al)} = \gamma_{(H)} B_{1(H)}$$

ensuring a non-selective pulse. Unless otherwise recorded in the text, all CP spectra were acquired with the parameters in parentheses (^{27}Al 90° pulse width, 4 μs; contact time, 0.3 ms; acquisition time, 1.022 s; sweep width, 100 kHz; time domain data size, 2048 words; maximum number of acquisitions, 3400).

2.2. X-Ray diffraction

Samples of the cement pastes which had been soaked in sodium chloride solution were dried, crushed and sieved to a fine powder for X-ray diffraction measurements. Diffraction patterns were obtained using a Philips diffractometer (PW1049) with a proportional counter (PW1965), with the samples contained in an aluminium holder covered with adhesive tape. The

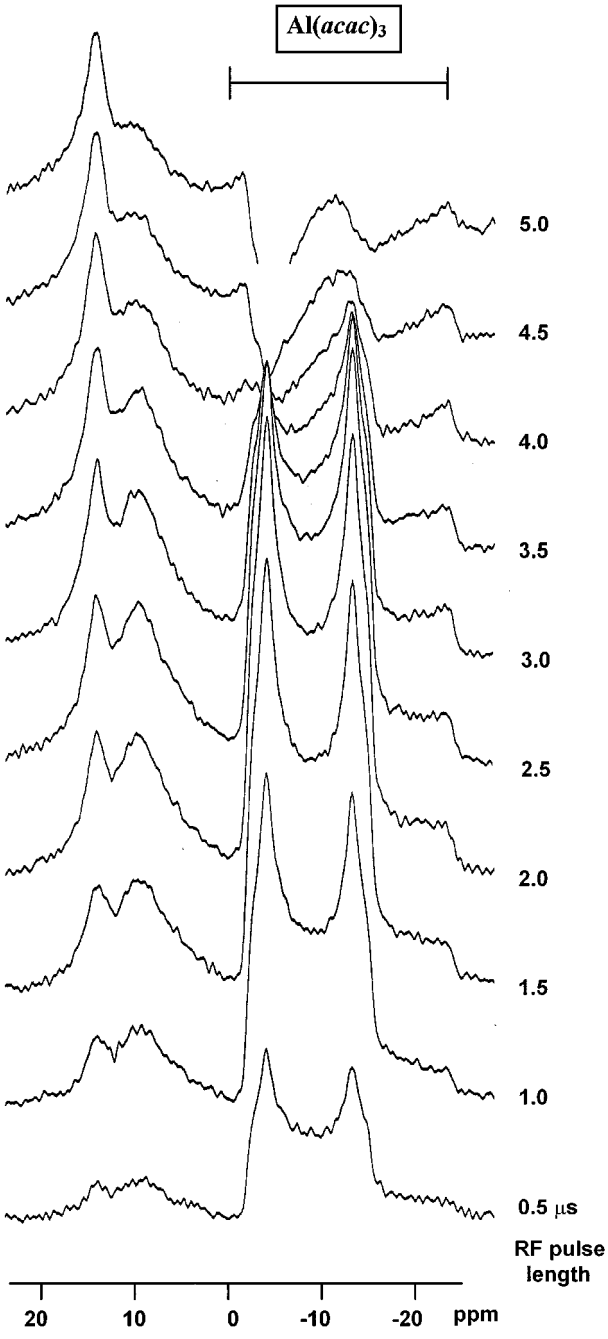

Figure 2 78.17 MHz ^{27}Al-{^{1}H} *pda* MAS solid state NMR spectrum of hydrated ***pc*** mixed with Al(*acac*)$_3$, obtained with a constant ^{27}Al power level $\omega_{rf} \approx 62$ kHz, but with the rf pulse length t_p varying from 0.5 to 5.0 μs, corresponding to flip angles from 11° to 110°.

generator (PW1010) was set at 40 kV and 20 mA, using Cu K_α radiation and a Ni filter. Scans were taken over a 2θ angular range of 5 to 70° with a step size of 0.1°.

3. Results and discussion

3.1. Hydration of the Portland cement/pozzolanic binder mixes

The main aluminate phases of unhydrated ***pc*** are C_3A and C_4AF. Some calcium sulphate, usually in the form of gypsum ($CaSO_4 \cdot 2H_2O$), is normally added to commercial ***pc*** to prevent 'flash setting', in which there is a rapid set, accompanied by much evolution of heat, and the subsequent development of strength is poor. It is associated with increased early reaction of the aluminate and ferrite phases and with the formation of a network of plates of AFm phases throughout the paste [20]. The mechanism of hydration of the calcium aluminates is generally accepted to be 'through solution', i.e. by dissolution of the anhydrous phases, followed by precipitation of the hydrates from solution [21] .

In the *absence* of calcium sulphate, the first hydration product is a gel-like material which grows at the C_3A surface and later transforms into hexagonal crystals corresponding to phases C_2AH_8 (strätlingite) and C_4AH_{19}. In the presence of calcium hydroxide the rate of hydration slows and only C_4AH_{19} forms as the primary product and then eventually converts to C_3AH_6. C_2AH_8 and C_4AH_{19} belong to the broad group of AFm phases¶ of general composition $[Ca_2(Al,Fe)(OH)_6]X \cdot xH_2O$ where X is a singly charged anion or half a formula unit of a doubly charged anion.

The AFm hydrates have a stacked layered structure which resembles the crystalline structure of portlandite but in which one Ca^{2+} out of three in a layer $Ca(OH)_2$ is replaced by an Al^{3+} ion in an ordered manner, causing an ionic charge imbalance in each 'principal layer', $[Ca_2Al(OH)_6 \cdot 2H_2O]^+$ [22]. The principal layers are stacked so as to produce octahedral cavities formed from three water molecules from each of the adjacent layers. These cavities may contain X anions, water molecules, or both [22a]. The anions in the interlayers of AFm phases are particularly prone to ion exchange [23]. In Friedel's salt, each cavity contains a Cl^- ion; in C_4AH_{13}, all contain one hydroxyl anion and one water molecule; C_4AH_{19} is structurally derived from C_4AH_{13} by the addition of an extra layer of water molecules [22a].

When the C_3A component of ***pc*** is hydrated in the *presence* of calcium sulphate, there is a reduction in the amount of C_3A hydrolysed in the initial stages. The AFt phase* ettringite (trisulphate) $C_6A\bar{S}_3H_{32}$ is formed as the main product of hydration.

$$C_3A + 3C\bar{S}H_2 = C_6A\bar{S}_3H_{32}$$

Minor amounts of calcium mono-sulphoaluminate $C_4A\bar{S}H_{12}$, or even C_4AH_{19}, may also be formed if an imbalance exists between the reactivity of C_3A and the dissolution rate of $CaSO_4$, resulting in an insufficient supply of SO_4^{2-} ions. After a rapid initial reaction, the hydration rate slows. The length of this dormant period may vary and increases with increasing amounts of calcium sulphate in the original paste. A faster hydration gets under way after all the available calcium sulphate is consumed, when the ettringite reacts with additional C_3A to give calcium mono-sulphoaluminate $C_4A\bar{S}H_{12}$,

$$C_6A\bar{S}_3H_{32} + 2C_3A + 4H = 3C_4A\bar{S}H_{12}$$

As ettringite is gradually consumed, hexagonal calcium aluminate hydrate C_4AH_{19} starts to form. It may be

¶ (Aluminate Ferrite mono-). The term 'mono' relates to the single formula unit of CaX_2 in another way of writing the formula: $C_3(A,F) \cdot CaX_2 \cdot yH_2O$.

* (Aluminate Ferrite tri-). The term 'tri' relates to the single formula unit of CaX_2 in another way of writing the formula: $C_3(A,F) \cdot 3CaX \cdot zH_2O$, where X is a doubly charged anion.

present as a solid solution with $C_4A\bar{S}H_{12}$, or as separate crystals. At ambient temperature, nearly complete hydration of the C_3A in ***pc*** pastes is attained within several months, depending, among other factors, on the water: solids ratio [24]. Calcium mono-sulphoaluminate C_4ASH_{12} is an AFm phase in which one half of the interlayer cavities contain SO_4^{2-} anions and the remainder contain two water molecules [22a]. The structure of ettringite, $C_3A{\cdot}3CaSO_4{\cdot}32H_2O$, is based on columns of empirical formula $[Ca_3Al(OH)_6{\cdot}12H_2O]^{3+}$, composed of $Al(OH)_6$ octahedra alternating with triangular groups of edge-sharing CaO_8 polyhedra, with which they share OH^- ions. The channels contain four sites, three occupied by sulphate and one by two water molecules. Exchange of sulphate by singly charged anions would appear to be unfavoured [22a].

It is generally accepted that, with the exception of ***pc***/***ggbs***, the reaction products resulting from the hydration of pozzolanic cements are the same as those occurring in Portland cement pastes [25]. The differences solely involve the ratios of the various compounds as well as their morphology. Others have identified, by a variety of techniques, the relatively few aluminate hydrates found in the hardened pastes as: ettringite; tetracalcium aluminate hydrate; calcium mono-sulphoaluminate; and strätlingite [26]. In the hydration of ***ggbs*** there is some evidence that the nature of the phases formed depends on the activator, which when that is ***pc*** can additionally produce hydrotalcite-type aluminate-containing phases as well as the usual AFm and AFt species [25]. Hydrotalcite-type phases are structurally related to brucite as the AFm phases are to *CH*, i.e. some of the Mg^{2+} ions are replaced by Al^{3+} and/or Fe^{3+} and the charge is balanced by anions, which together with water molecules, occupy interlayer sites [27].

The chemical shift range of ^{27}Al is quite small, four-coordinated aluminium resonating between 80 and 50 ppm; six-coordinated aluminium between 20 and −20 ppm. Broadened lines may limit the resolution with the effect that chemically inequivalent sites may not be resolved. It might be expected that dipolar interactions would be small compared with the quadrupolar interactions but we have found that high-power proton decoupling can lead to useful reductions in the line widths of the central transition observed in the ^{27}Al spectra of *hydrated* Portland cement mixes. Others have reported similar line narrowing in the ^{27}Al-$\{^1H\}$ solid state NMR spectra of cements [14, 28].

The ^{27}Al MAS spectra of the *anhydrous* Portland cement mixes are shown in Fig. 3. High power ^1H decoupling did not lead to any reduction in line width for any of the resonances and no signal was obtained with CP/MAS. None of the anhydrous cement mixes showed indications of six-coordinated aluminium, and in the case of ***pc***/***pfa*** there was an intense and extensive manifold of spinning side bands, indicative of strongly anisotropic (electric and/or magnetic) local environments for the aluminium nuclei. In all cases, hydration led to the rapid appearance of six-coordinate aluminium solid phases and after only three days relatively little four co-ordinated aluminium remained. However, it should be noted that other workers have shown that ^{27}Al NMR spectroscopy can detect the presence of some four co-ordinated aluminium in substituted calcium silicate hydrate gels, related by morphology and by composition to the gels present in blast-furnace slag/Portland cement blends [29]. Indeed, in the *pda* (but not the CP/MAS) spectrum of hydrated ***pc***/***ggbs*** we observed a minor peak in the region expected for tetrahedral aluminium. However, it tended to become less intense with increasing time after hydration (Fig. 4), indicating that substitution into the calcium silicate gel was not a major fate for most of the aluminium on hydration of this particular cement paste.

In contrast to the anhydrous samples, CP/MAS spectra were observed for all of the hydrated species and, while the signals were generally narrower compared with the corresponding *pda* spectra, the spectra could also be satisfactorily interpreted without invoking the presence of any additional aluminate phases.

Spectral assignments were made only for six-coordinate (hydrated) aluminium species, although because of the many overlapping spinning side bands it was not considered practicable to disentangle and simulate individual manifolds to obtain C_Q and η values as an aid to spectral assignment [8]. While Faucon *et al.* have recently used an alternative technique of triple quantum MAS spectroscopy very successfully to obtain these parameters for some *pure* calcium aluminate hydrate phases [11], in the present study of multi-component *cement pastes*, the hydrated aluminate species were identified only by the chemical shifts and very characteristic widths of their signals, deconvoluted as simple Gaussian lines. As already indicated above, such an approximation becomes less valid with increasing line width.

Ettringite, $C_6A\bar{S}_3H_{32}$, and Friedel's salt (only observed when the samples were soaked in NaCl solution) gave narrow signals; tetracalcium aluminate hydrate, C_4AH_x, gave a signal of intermediate width; calcium mono-sulphoaluminate, $C_4A\bar{S}H_{12}$, gave the broadest signal in the *pda* spectra. This last signal was much reduced in intensity and width in the CP spectra[†], suggesting that mono-sulphoaluminate has different types of Al sites, at least one of which is relatively distant from potentially cross polarising ^1H's. Others have already commented that for C_4ASH_{12} the observed spinning side band pattern from the satellite transitions cannot be described by a single set of C_Q, η values [8]. The basic spectral parameters used to make the assignments were obtained from either literature values in the cases of ettringite and calcium mono-sulphoaluminate [8] or authentic samples in the cases of tetracalcium aluminate hydrate and Friedel's salt (this work). The basic spectral parameters were used as starting points and the ranges of chemical shifts and line widths obtained

[†] The intensity of an ^{27}Al signal in a CP spectrum is dependent on the relation between contact time, proton $T_{1\rho}$ (which is determined by low frequency movements of water molecules), and cross polarisation time (determined mainly by the distance between ^1H's and polarised ^{27}Al nuclei). Also a fast repetition of CP cycles may cause a selective suppression of the magnetisation of slowly relaxing ^1H's, hence affecting the efficiency of cross polarisation [21c].

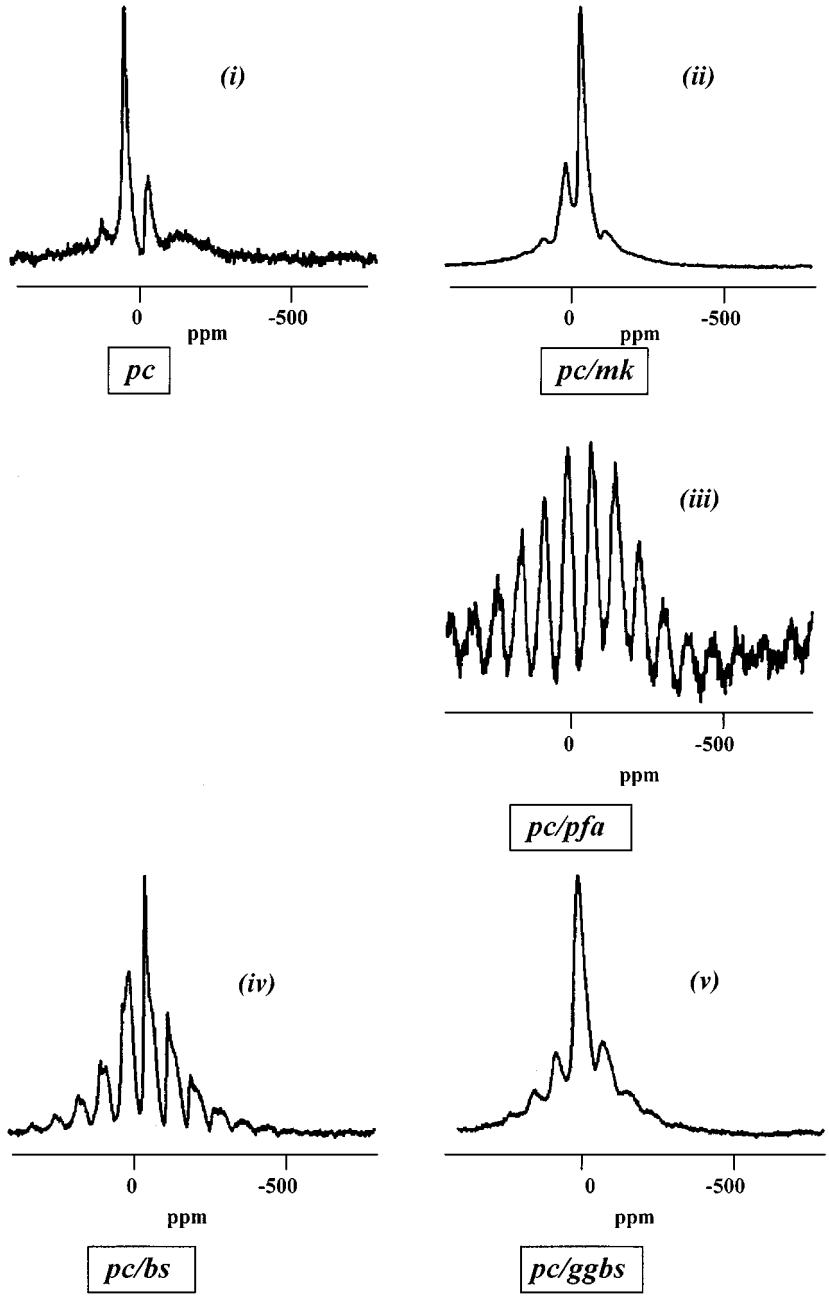

Figure 3 78.17 MHz ^{27}Al MAS NMR spectra of the cement paste *anhydrous* binders: (i) ***pc***; (ii) ***pc/mk***; (iii) ***pc/pfa***; (iv) ***pc/bs***; (v) ***pc/ggbs***.

from the actual spectral deconvolutions are recorded in Table II. We consider that the Gaussian assumption was justified given the remarkably (for ^{27}Al spectra) narrow and symmetric signals observed, especially for ettringite and tetracalcium aluminate hydrate, suggesting that second order quadrupolar effects were small. All of the cement blends gave remarkably consistent ν_{cg}, $\nu_{1/2}$, and ν_{iso} values for the deconvoluted spectral components, by far the largest variation occurring for that assigned to calcium mono-sulphoaluminate (*pda* spectra: ν_{cg}, 10.9 ± 2.7; $\nu_{1/2}$, 14.7 ± 5.8; ν_{iso}, 23.6 ± 6.8 ppm. CP/MAS spectra ν_{cg}, 10.6 ± 1.9; $\nu_{1/2}$, 6.9 ± 2.0; ν_{iso}, 16.6 ± 3.4 ppm.). Observed and deconvoluted ^{27}Al *pda* and CP/MAS spectra and their assignments are shown in Figs 5(i) and 6(i) respectively. As a general rule, only the minimum number of deconvoluted peaks necessary to give satisfactory fit to the observed, rather featureless, spectra was accepted and their chemical shifts (ν_{cg}), widths ($\nu_{1/2}$), and adjusted isotropic chemical shifts (ν_{iso}) are recorded in Table III. The fit was adjudged satisfactory when the difference spectrum obtained by subtracting the calculated from the observed spectrum was indistinguishable from the projected base line. Only in those cases where it significantly improved the fit was a peak at the resonance frequency of C_4AH_x included in the deconvolution.

We consider that cross polarisation caused large underestimates in the relative contribution made by the $C_4A\bar{S}H_{12}$ phase to the overall spectrum and therefore was not applied when spectra were obtained for purposes of comparison.

Significant changes were observed in both the *pda* and CP/MAS spectra which were dependent on both spinning rate and for how long the sample was spun. Such changes have not been reported previously and

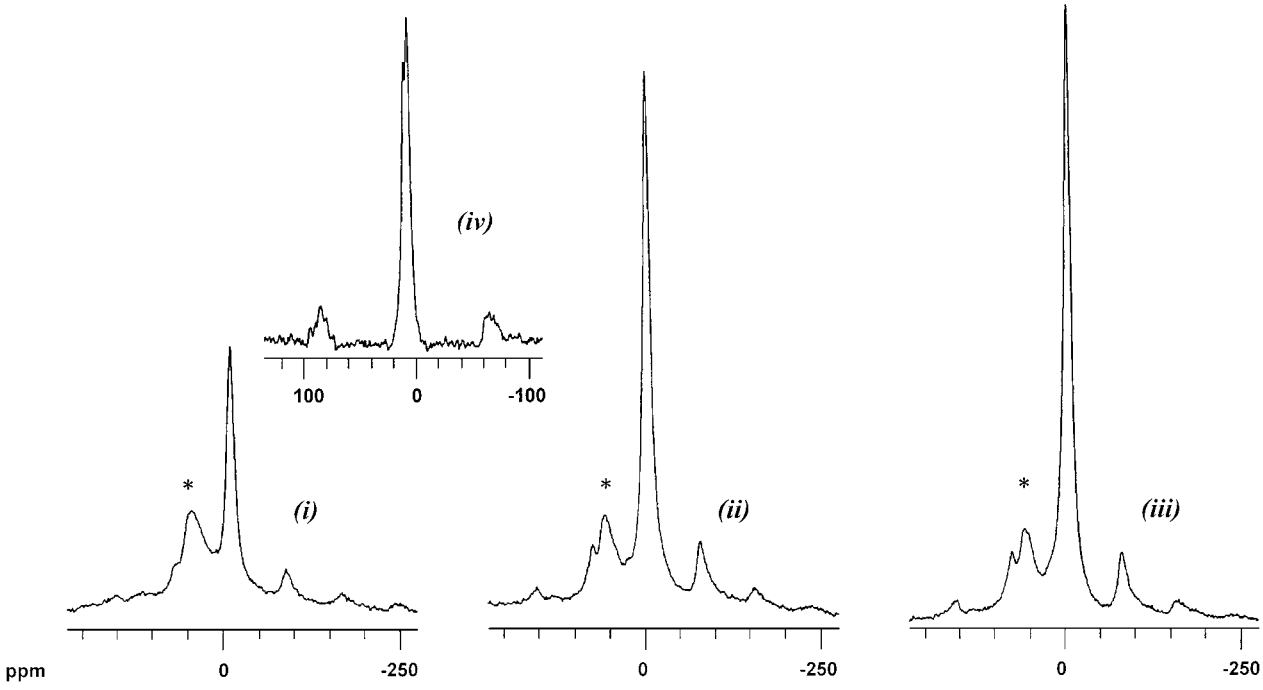

Figure 4 78.17 MHz ^{27}Al-{^{1}H} MAS solid state NMR of the ***pc/ggbs*** cement paste after (i) 3 days'; (ii) 1 month's; (iii) 6 months' hydration (peak marked * is due to Al_{tet}). (iv) CP/MAS spectrum after 6 months' hydration.

TABLE II 78.17 MHz ^{27} Al-{^{1}H} solid state NMR spectra: chemical shifts (observed, ν_{cg}, ppm; adjusted isotropic, ν_{iso}, ppm) and line widths ($\nu_{1/2}$, ppm) used to make assignments of aluminate phases of the cement paste samples

	ν_{cg} ppm	$\nu_{1/2}$ ppm	ν_{iso} ppm
pda[a]			
$C_6A\bar{S}_3H_{32}$[b]	13.8 ± 0.3	2.1 ± 0.8	15.9 ± 0.8
$C_4A\bar{S}H_{12}$[c]	10.9 ± 2.7	14.7 ± 5.8	23.6 ± 6.8
C_4AH_x[d]	9.3 ± 0.7	3.4 ± 0.1	12.3 ± 0.8
Friedel's Salt	9.1 ± 0.4	1.9 ± 0.3	10.6 ± 0.7
	7.9 ± 0.3	2.4 ± 0.6	10.1 ± 0.8
cp[e]			
$C_6A\bar{S}_3H_{32}$	13.6 ± 0.3	2.1 ± 0.4	15.6 ± 0.3
$C_4A\bar{S}H_{12}$	10.6 ± 1.9	6.9 ± 2.0	16.6 ± 3.4
C_4AH_x	9.4 ± 0.5	4.3 ± 1.1	13.3 ± 1.1
Friedel's Salt	8.9 ± 0.5	1.7 ± 0.2	10.2 ± 0.6
	7.9 ± 0.5	2.3 ± 0.4	9.7 ± 0.3

[a]78.17 MHz ^{27}Al-{^{1}H} spectra; [b]ettringite; [c]calcium mono-sulphoaluminate; [d]tetracalcium aluminate hydrate; [e]CP/MAS spectra (same samples).

appeared to reflect *chemical* changes caused by the pore fluids being forced from the samples *via* the open continuous pore system under the effects of the high centrifugal force resulting from magic angle spinning. Fig. 7 shows the ^{27}Al CP/MAS spectrum of the same bulk sample of hydrated ***pc*** observed at one hourly intervals while being continuously spun at 2.5 and 6.0 kHz for 20 hours in a 7.5 mm o.d. rotor. At the higher spinning rate, significant changes occurred in both the total integral of all peaks (spinning side bands included) and the relative integrals of the signals at their ν_{cg}'s, whereas the spectrum obtained at 2.5 kHz remained more or less unchanged even after 20 hours spinning. That significant spectral changes were dependent only on spinning rate indicated that the observed effects were not merely the result of loss of water associated with drying of the sample. The *pda* spectrum of hydrated ***pc*** spun at 4.2 kHz over a period of several hours (Fig. 8) also showed changes in the relative integrals of the signals at their ν_{cg}'s, but not in the total integral for all peaks when their spinning side bands were included. The fully relaxed *pda* spectrum should give the relative concentrations of the aluminate phases present after any spinning time, provided that a selective (π/12) exciting pulse is used and that the manifold of spinning side bands can be disentangled and their contributions appropriately assigned to individual aluminate phases. There was, however, little point in attempting to achieve the quantitatively reliable spectra resulting from very short selective pulses as the necessarily increased spinning times themselves resulted in significant actual changes in the relative concentrations of the aluminate phases.

We therefore considered it important to obtain MAS spectra at the lowest spinning rate consistent with the need to retain between the spinning side bands observational 'windows' for the signals at their ν_{cg}'s, and in the shortest possible acquisition times ($\leq$30 minutes spinning time for a *pda* spectrum); i.e. using a non-selective (compromise $\sim\pi/2$) pulse to give optimum signal:noise for the central transitions. Moreover, the porosity of a hardened ***pc*** paste generally increases with increasing initial water:cement ratio and spectral comparisons were therefore only made for samples prepared with the same w/c ratio (0.4), although it should also be noted that the presence of pozzolanas changes the porosities of ***pc*** pastes, even those prepared with the same w/c ratio. Care was therefore taken to ensure that spectra obtained for comparison purposes were all observed for samples spun at the same rate (ω_r, 4.2 kHz) and for the same period of time which was kept as short as was consistent with the acquisition of sufficient scans to give an acceptable signal:noise.

TABLE III 78.17 MHz ^{27}Al-{^{1}H} solid state NMR spectra: chemical shifts (observed, ν_{cg}, ppm; adjusted isotropic, ν_{iso}, ppm) and line widths ($\nu_{1/2}$, ppm) of the deconvoluted signals assigned to the aluminate phases of the cement paste samples

	pc			***pc/sf***			***pc/ls***			***pc/mk***			***pc/bs***			***pc/pfa***			***pc/ggbs***			Mean		
	ν_{cg}	$\nu_{1/2}$	ν_{iso}	ν_{cg}	$\nu_{1/2}$	ν_{iso}	ν_{cg}	$\nu_{1/2}$	ν_{iso}	ν_{cg}	$\nu_{1/2}$	ν_{iso}	ν_{cg}	$\nu_{1/2}$	ν_{iso}	ν_{cg}	$\nu_{1/2}$	ν_{iso}	ν_{cg}	$\nu_{1/2}$	ν_{iso}	ν_{cg}	$\nu_{1/2}$	ν_{iso}
pda[a]																								
$C_6A\bar{S}_3H_{32}$ (H_2O)[b]	13.7	1.7	15.2	13.8	2.9	16.4	14.1	2.9	16.7	13.9	1.3	15.1	13.7	1.5	15.0	13.8	2.1	15.7	13.7	2.1	15.6	13.8	2.1	15.7
$C_6A\bar{S}_3H_{32}$ (NaCl)[c]	13.5	2.0	15.3	13.8	2.1	15.7	13.5	2.9	16.1	13.6	1.6	15.0	13.8	2.2	15.8	13.8	2.3	15.9	13.7	1.9	15.6	13.7	2.1	15.6
$C_4A\bar{S}H_{12}$ (H_2O)[d]	13.5	10.3	22.3	11.6	16.2	26.1	12.1	20.4	30.3	12.8	9.3	21.1	12.2	11.6	22.6	11.8	13.5	23.9	8.8	9.5	17.3	12.1	12.7	23.5
$C_4A\bar{S}H_{12}$ (NaCl)[e]	12.3	10.0	20.8	9.8	13.1	21.5	11.3	19.8	29.0	12.3	8.9	20.3	9.6	12.1	20.4	12.0	13.1	23.7	8.2	9.6	16.8	11.2	12.0	21.9
C_4AH_x (H_2O)[f]	8.7	3.4	11.7	—	—	—	—	—	—	9.2	3.5	12.3	8.0	2.9	10.6	—	—	—	10.0	3.5	13.1	8.6	3.3	11.5
C_4AH_x (NaCl)[g]	—	—	—	—	—	—	—	—	—	—	—	—	—	—	—	—	—	—	—	—	—	—	—	—
F. S. (NaCl)[h]	8.7	1.7	10.2	9.0	1.0	9.9	9.4	2.0	11.2	9.0	1.5	10.3	8.8	1.6	10.2	9.0	1.1	10.0	8.8	2.0	10.6	9.0	1.5	10.3
	7.8	2.2	9.8	8.2	1.8	9.8	8.2	3.0	10.9	8.0	1.9	9.7	7.6	1.8	9.2	8.0	1.9	9.7	7.8	2.5	10.0	7.9	2.2	9.9
cp[i]																								
$C_6A\bar{S}_3H_{32}$ (H_2O)	13.7	1.8	15.3	13.3	2.5	15.5	n.a.	n.a.	n.a.	13.8	1.7	15.3	13.5	2.2	15.5	13.6	2.5	15.8	13.6	2.2	15.6	13.6	2.2	15.5
$C_6A\bar{S}_3H_{32}$ (NaCl)	13.8	1.8	15.4	13.3	2.5	15.5	n.a.	n.a.	n.a.	13.3	2.2	15.3	n.a.	n.a.	n.a.	13.5	2.3	15.6	13.3	2.3	15.4	13.4	2.2	15.4
$C_4A\bar{S}H_{12}$ (H_2O)	—	—	—	12.4	7.8	19.4	n.a.	n.a.	n.a.	—	—	—	11.8	5.0	18.2	12.2	7.5	18.9	8.7	5.0	13.2	12.1	6.8	18.8
$C_4A\bar{S}H_{12}$ (NaCl)	10.8	6.8	16.6	10.8	7.6	17.6	n.a.	n.a.	n.a.	—	—	—	n.a.	n.a.	n.a.	12.0	8.8	19.9	9.2	6.0	14.6	11.6	7.1	17.9
C_4AH_x (H_2O)	9.5	3.7	12.8	—	—	—	n.a.	n.a.	n.a.	8.9	3.9	12.4	9.1	4.4	13.0	9.5	5.3	14.2	9.9	3.2	12.8	9.3	4.3	13.1
C_4AH_x (NaCl)	—	—	—	—	—	—	n.a.	n.a.	n.a.	—	—	—	n.a.	n.a.	n.a.	—	—	—	—	—	—	—	—	—
F.S. (NaCl)	9.3	1.5	10.6	8.4	1.6	9.8	n.a.	n.a.	n.a.	9.1	1.9	10.8	n.a.	n.a.	n.a.	8.5	1.6	9.9	8.6	1.7	10.0	8.8	1.5	10.2
	8.3	1.9	10.0	7.6	1.9	9.3	n.a.	n.a.	n.a.	8.1	2.1	9.9	n.a.	n.a.	n.a.	7.6	2.0	9.4	7.4	2.7	10.0	7.8	2.0	9.7

[a] ^{27}Al-{^{1}H} spectrum; [b] ettringite, hydrated sample; [c] ettringite, hydrated then soaked in 5M NaCl; [d] calcium mono-sulphoaluminate, hydrated sample; [e] calcium mono-sulphoaluminate, hydrated then soaked in 5M NaCl; [f] tetracalcium aluminate hydrate, hydrated sample; [g] tetracalcium aluminate hydrate, hydrated then soaked in 5M NaCl; [h] Friedel's salt, sample soaked in 5M NaCl; [i] CP/MAS spectrum.

Skibsted *et al.* have convincingly assigned the two resonances observed in the ^{1}H-decoupled MAS spectrum of hydrated ***pc*** to ettringite (narrower signal) and calcium mono-sulphoaluminate (broader) [8]. We find that with the present ***pc*** samples there is a rather better fit of deconvoluted to observed spectra if a small quantity of C_4AH_x is assumed to be also present. For all the samples investigated the *pda* spectra could be assigned satisfactorily without invoking the presence of any hydrated aluminate phases other than ettringite, calcium mono-sulphoaluminate, and tetracalcium aluminate hydrate.

With increasing hydration time the intensity of the signal assigned to ettringite decreased significantly relative to those of the signals assigned to mono-sulphoaluminate and calcium aluminate hydrate(s) and after six months the integrals in the *pda* spectra were in the ratios recorded in Table IV. It should be emphasised that these ratios were obtained by comparisons of the integrals of the central transitions only and do not include any contributions from the spinning sidebands. Neither do they necessarily give the relative *concentrations* of the aluminate solid phases in a given sample. Nevertheless, as all the spectra were obtained under the same acquisitional regime, comparisons of the ratios between the signal integrals of the constituent phases observed for different samples should still be valid. As might therefore be anticipated [26], although the binders were compositionally heterogeneous, after hydration the aluminate phases present, but not their relative proportions, were similar: a rapid dissolution of four co-ordinated aluminium species led to the precipitation of ettringite,

TABLE IV Ratios of the integrals of the deconvoluted signal assigned to aluminate phases observed in the 78.17 MHz ^{27}Al-{^{1}H} solid state *pda* NMR spectra of the cement paste samples

Aluminate phase	***pc***		***pc/sf***		***pc/ls***		***pc/mk***		***pc/pfa***		***pc/bs***		***pc/ggbs***	
	H_2O	NaCl	H_2O	NaCl	H_2O	NaCl	H_2O	NaCl	H_2O	NaCl	H_2O	NaCl	H_2O	NaCl
$C_6A\bar{S}_3H_{32}$[a]	16	137	49	57	45	8	14	158	<1	6	4	<1	4	4
$C_4A\bar{S}H_{12}$[b]	100	100	100	100	100	100	100	100	100	100	100	100	100	100
C_4AH_x[c]	9	—	—	—	—	—	25	—	—	—	11	—	89	—
F.S.[d]	—	80	—	13	—	23	—	223	—	76	—	8	—	101

[a] ettringite; [b] calcium mono-sulphoaluminate; [c] calcium aluminate hydrate; [d] Friedel's salt.

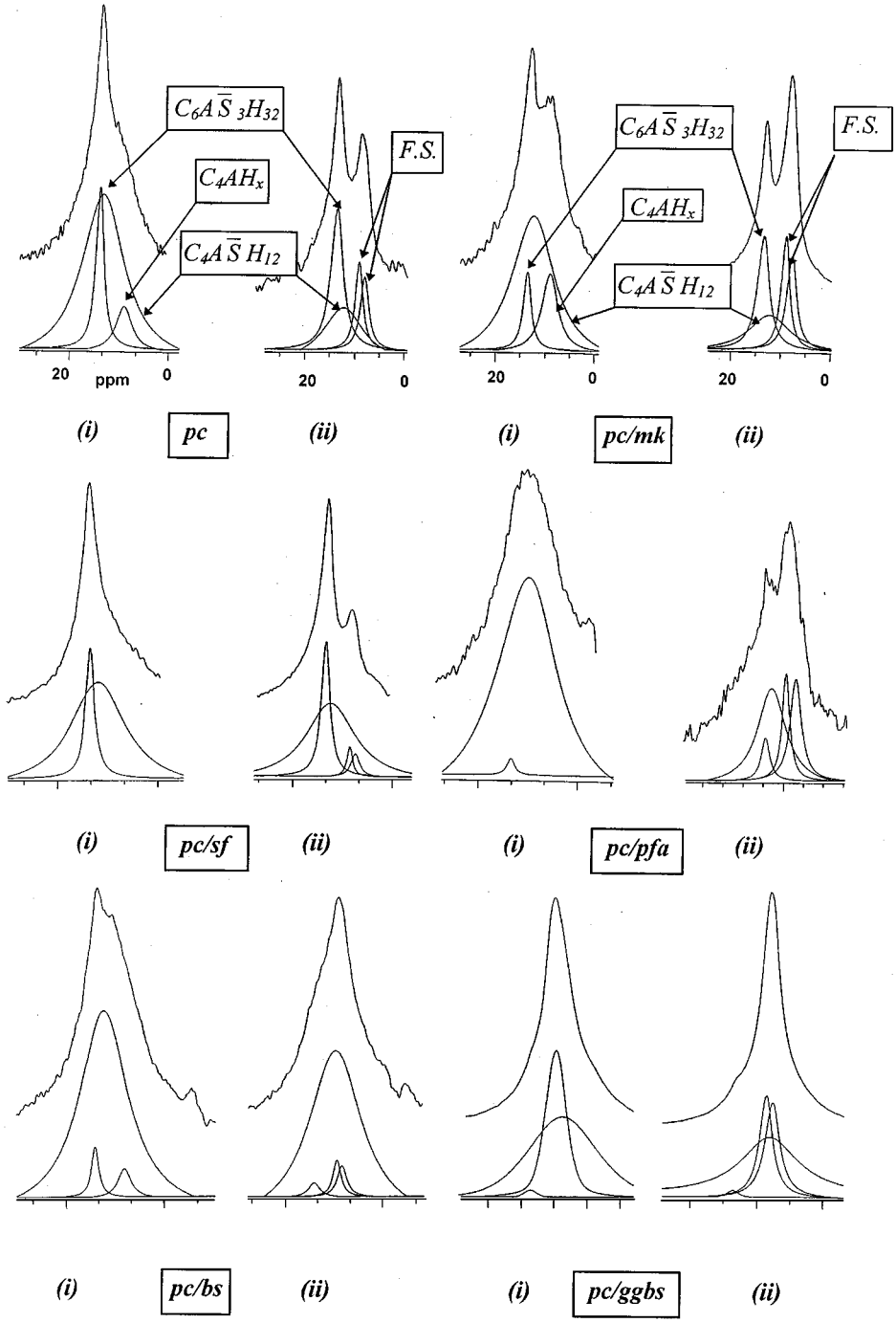

Figure 5 78.17 MHz ^{27}Al-{^{1}H} *pda* MAS solid state NMR spectra of the cement pastes; (i) after 6 months' hydration; (ii) after 6 months' hydration followed by 6 months' soaking in 5M NaCl solution.

followed by a slower conversion to $C_4A\bar{S}H_{12}$ and calcium aluminate hydrate(s). Hence the calcium deficient binders ***pfa***, ***mk*** and ***bs*** gave particularly high AFm : AFt ratios, with little residual ettringite, but so also did the calcium rich ***ggbs***. The presence of either ***sf*** or ***ls*** caused significant *decreases* in the AFm : AFt ratio compared with ***pc*** on its own.

3.2. Chloride binding in the Portland cement/pozzolanic binder mixes

Six months after initial hydration, ***pc/pozzolana*** cement cubes were soaked in 5M NaCl solution for up to a further 6 months, when specimens were prepared for spectroscopy. For all the samples investigated, both the *pda* and CP/MAS spectra could be assigned satisfactorily without invoking the presence of any hydrated aluminate phases other than ettringite, calcium mono-sulphoaluminate, tetracalcium aluminate hydrate(s) and Friedel's salt, $C_3A{\cdot}CaCl_2{\cdot}10H_2O$. Observed and deconvoluted ^{27}Al *pda* and CP/MAS spectra and their assignments are shown in Fig. 5(ii) and 6(ii) respectively. We confirmed the presence of Friedel's salt by XRD measurements on the cement paste samples which showed the presence of reflections at those angles observed by ourselves for an authentic sample and as reported by others [30].

Fig. 5(ii) and Table IV show that in the *pda* spectra for all the samples except ***pc/ls*** and ***pc/bs*** the intensity of the signal arising from mono-sulphoaluminate fell relative to that from ettringite, which appeared also to remain more constant post soaking the cured cement

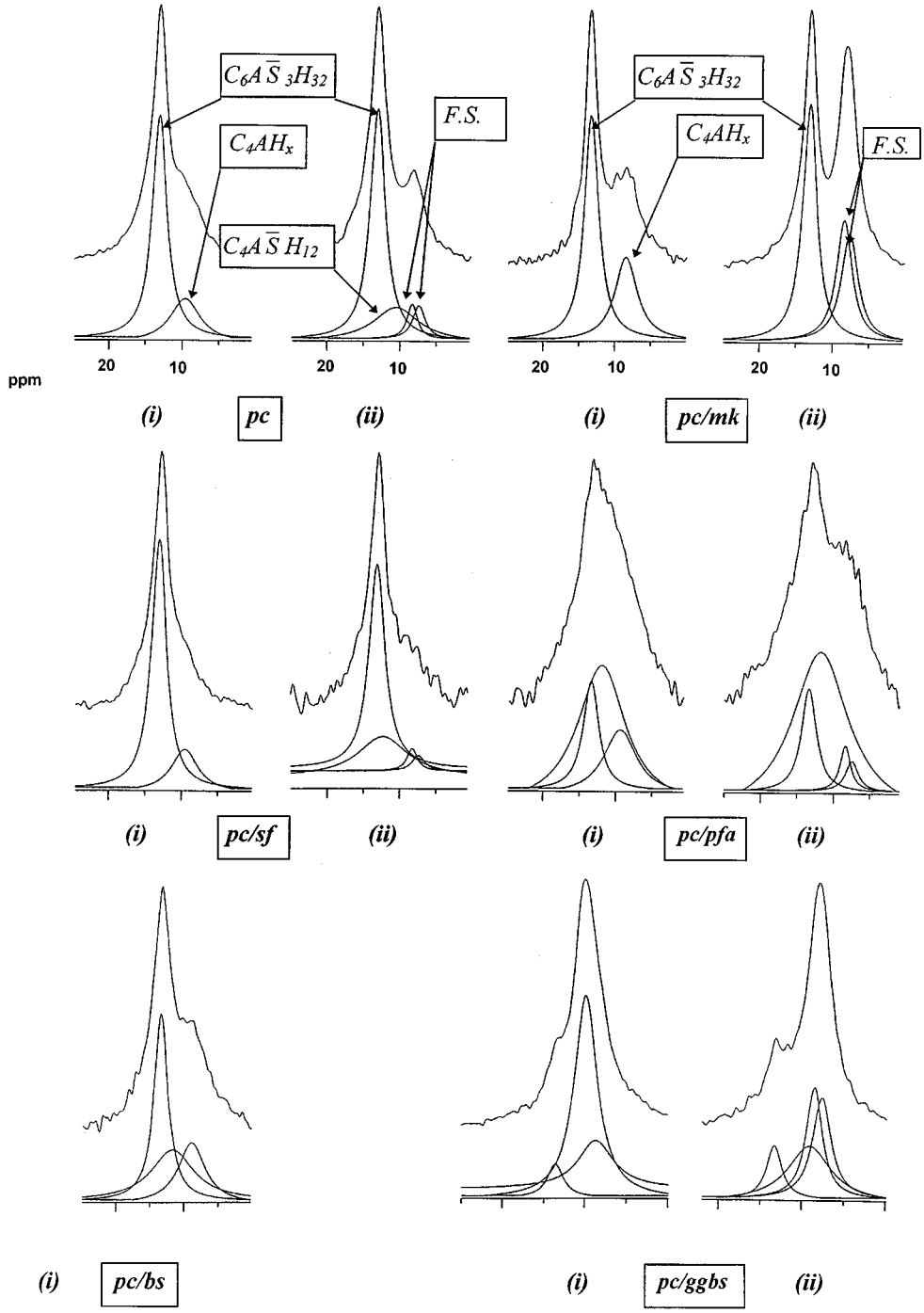

Figure 6 78.17 MHz ^{27}Al-{^{1}H} CP/MAS solid state NMR spectra of the cement pastes; (i) after 6 months' hydration; (ii) after 6 months' hydration followed by 6 months' soaking in 5M NaCl solution.

pastes in NaCl solution. A signal assigned to C_4AH_x was no longer needed to assure acceptable deconvolution of the spectra. The fall in the relative intensity of the signal from $C_4A\bar{S}H_{12}$ was partially compensated for by the appearance of the two signals assigned to Friedel's salt. Compared with ***pc*** alone (1 : 1.7), the Friedel's salt : ettringite ratio was much higher for ***pc/sf*** (1 : 4.4), but significantly lower for ***pc/ls*** (1 : 0.3). With the exception of ***pc/bs***, those binders with the highest AFm : AFt ratios in the spectrum of the purely hydrated sample also had the highest Friedel's salt : ettringite ratios post soaking in NaCl solution. The highest ratios occurred for ***pc/mk*** (1.4 : 1), ***pc/pfa*** (12.7 : 1) and ***pc/ggbs*** (>80 : 1).

The key to the formation of the chemically robust Friedel's salt appears to be high concentrations of the AFm phase(s) calcium mono-sulphoaluminate and/or calcium aluminate hydrate(s). Others have used pore solution analyses to study the mechanism of Friedel's salt formation in cements rich in tri-calcium aluminate, C_3A [22b]. Pore solutions from mortars containing NaCl and $CaCl_2$ added during mixing were analysed and it was concluded that in the presence of NaCl the Friedel's salt formed by two separate mechanisms: an adsorption mechanism, and an anion-exchange mechanism. A similar situation would appear to apply with the ***pc***-based binders of the present study, particularly given the propensity for

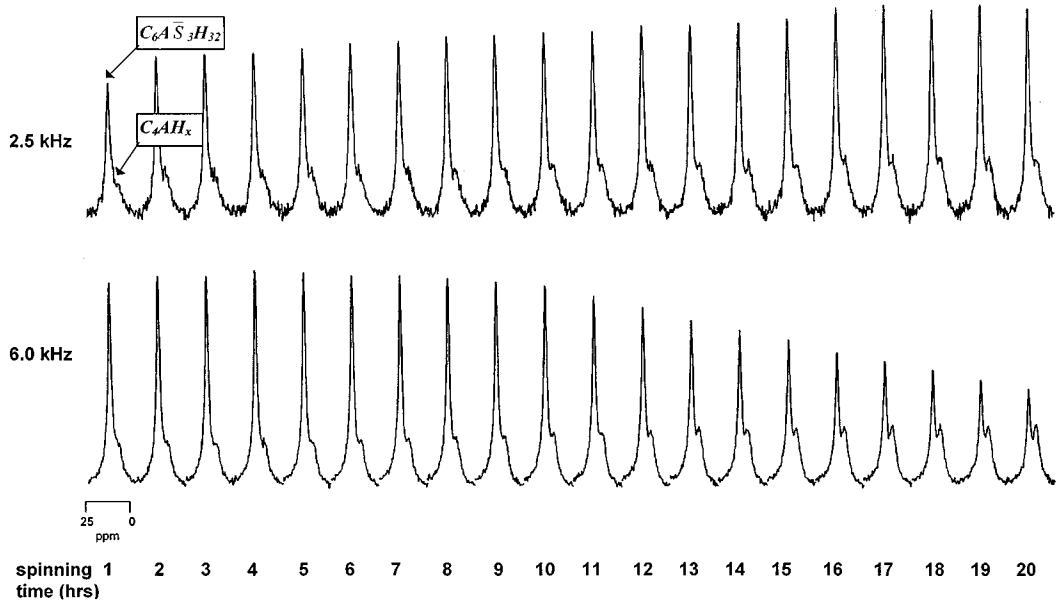

Figure 7 78.17 MHz ^{27}Al-{^{1}H} CP/MAS spectrum of a sample of hydrated ***pc*** observed at one hourly intervals while being continuously spun at 2.5 and 6.0 kHz for 20 hours in a 7.5 mm o.d. rotor.

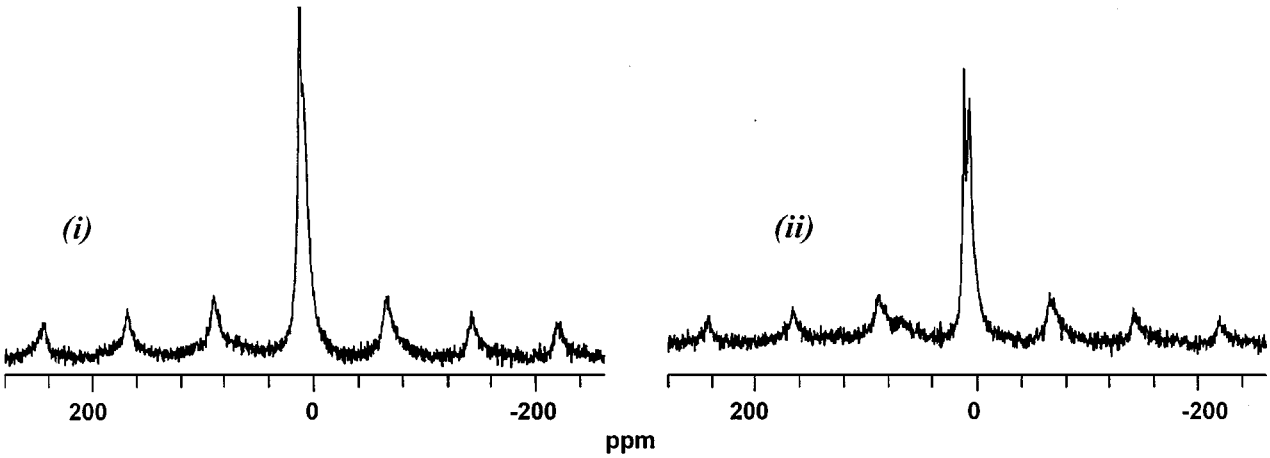

Figure 8 78.17 MHz ^{27}Al-{^{1}H} CP/MAS solid state NMR spectrum hydrated ***pc*** (i) after 0.5 hr; (ii) after 8 hrs'continuous spinning (ω_r, 4.2 kHz).

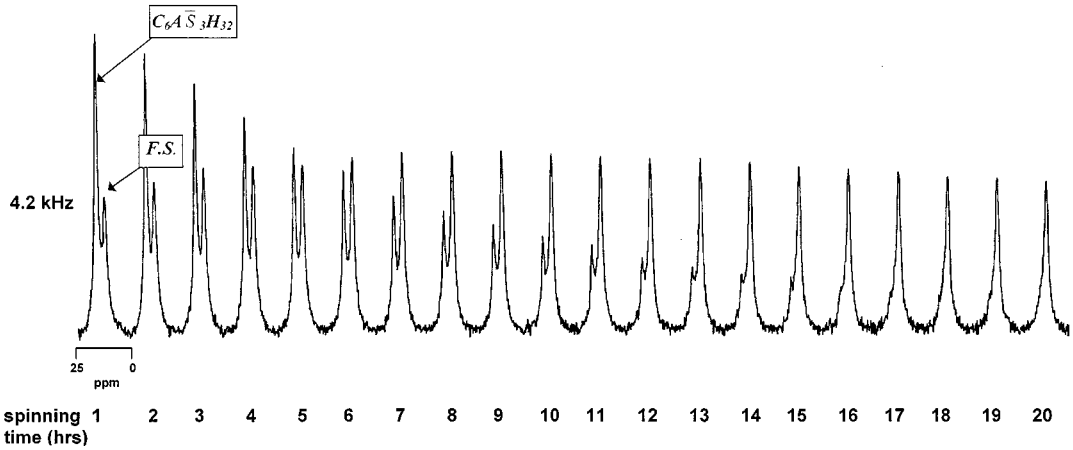

Figure 9 78.17 MHz ^{27}Al-{^{1}H} CP/MAS (ω_r, 4.2 kHz) of a hydrated sample of ***pc*** post soak in 5M NaCl solution sampled at hourly intervals during a 20 hour period when the sample was spun continuously.

hydroxyl ion exchange by AFm phases. The relative constancy of the signal arising from ettringite post soaking the sample in NaCl solution would also appear to be consistent with the relatively unfavourable exchange of sulphate by singly charged anions [22a].

As with the purely hydrated samples, significant changes were observed in both the *pda* and CP/MAS spectra which were dependent on both spinning rate and for how long the sample was spun. Fig. 9 shows the ^{27}Al CP/MAS spectrum (ω_r, 4.2 kHz) of a hydrated sample of ***pc*** soaked in 5M NaCl solution sampled at

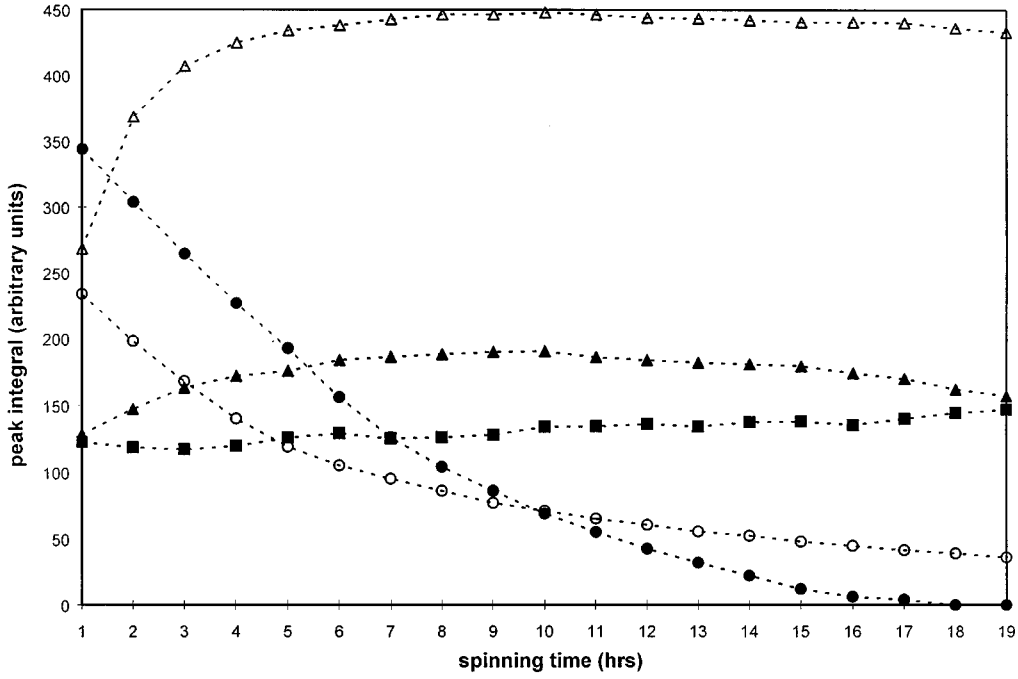

Figure 10 Plots of the integrals (arbitrary units) of the ν_{cg} signals (CP/MAS spectrum; ω_r, 4.2 kHz) assigned to ettringite (open circles) and calcium mono-sulphoaluminate (open triangles) for a hydrated (6 months) ***pc*** paste, and for the signals assigned to ettringite (filled circles), calcium mono-sulphoaluminate (triangles) and Friedel's salt (filled squares), for the same cured ***pc*** paste sample soaked in 5M NaCl solution (6 months). The samples were powdered and spun continuously for a period of 20 hours, with the spectra acquired at hourly intervals.

hourly intervals during the 20 hour period when the sample was spun continuously. As the local pH must have changed on expression of pore fluids then so, it appeared, did both the total integral of all peaks (spinning side bands included) and the ratios of aluminate species present. The ettringite signal intensity decreased monotonically with increasing spinning times, in contrast to that from Friedel's salt which increased before plateauing or falling away after about 9–10 hours, whereas the calcium mono-sulphoaluminate signal intensity remained relatively constant. The integrals of the ν_{cg} signals (CP/MAS spectrum) for ettringite, calcium mono-sulphoaluminate, and Friedel's salt, against spinning time for the same cured ***pc*** paste sample soaked in 5M NaCl solution, powdered and spun at 4.2 kHz for a period of 20 hours are plotted in Fig. 10. While an artefact of the spectral acquisition, this phenomenon did provide information about the effects of changes in pore fluids on the ratios of the aluminate components, particularly as the CP/MAS spectra consistently under-represented the concentration of mono-sulphoaluminate relative to the other aluminate phases. That the prolonged spinning of the sodium chloride soaked hydrated ***pc*** sample caused an apparent increase in the Friedel's salt : ettringite integral ratio, which was accompanied by a *reduction* in the total integral of all peaks, suggests that the ettringite had not changed directly to Friedel's salt but *via* the mono-sulphoaluminate phase.

4. Conclusions

As has been pointed out [8], $C_4A\bar{S}H_{12}$ is incorporated within the amorphous calcium silicate hydrate gel of ***pc***, is less ordered and therefore extremely difficult to detect by XRD or thermal analysis [8]. On the other hand, aluminoferrites cannot be detected by NMR. Nonetheless, provided that care is taken in spectral acquisition ^{27}Al *pda* and CP/MAS (particularly the former) are powerful techniques to study the aluminate phases in ***pc***-based cements. However, a complicating factor, not previously identified, is the effect on the relative concentrations of the aluminate phases caused by cement pore fluid expression as a result of the centrifugal forces imposed by magic angle spinning at high rotational rates.

With respect to concrete technology, the key outcome of this study, has been to confirm and clarify the rôles and interactions of Portland and non-Portland binders in modifying the degree of chloride binding as Friedel's salt. With the exception of ***pc/sf***, large increases in both the amount of mono-sulphoaluminate and the $C_4ASH_{12} : C_6AS_3H_{32}$ ratio occurred in the hydrated cement pastes when the pozzolanas were present, and it was the AFm phases which were the main precursors to Friedel's salt. The AFt phases have little or no capability for directly binding with chlorides. Although the binders were compositionally heterogeneous, after hydration the aluminate phases present in the cement pastes, but not their relative proportions, were found to be similar. The reason why different binders produced different AFm:AFt ratios is not yet clear but it appears that mono-sulphoaluminate phases were produced in high yield by those non-Portland binders which have 'reactive' calcium phases. Thus, based on the bulk oxide and modal compositions of the materials tested, blends of ***pc*** with ***mk***, ***pfa*** and ***ggbs*** are likely to be the most effective in producing AFm phases capable of binding chlorides. This capability is probably promoted by the large surface area of the ***mk***, the high calcium content of ***ggbs***, and that both ***ggbs*** and ***pfa*** can be used

to replace large proportions of ***pc*** in concrete mixes. The hypothesis also explains why ***sf***, ***ls*** and ***bs*** had relatively little effect on the AFm : AFt ratio, as these have little or none of the reactive calcium content needed to produce mono-sulphoaluminate development from ettringite. However, it should be noted that other factors, such as the local pH conditions, are also likely to influence the AFm : AFt ratio.

Nevertheless, ^{27}Al NMR spectroscopy can assist civil engineers in the selection of suitable binders to give durable concrete mixes for infrastructure exposed to chloride environments. It may even be possible eventually to assess the effectiveness of groups of binders to provide AFm phases and, thus indirectly, the chloride binding capacity of a particular mix. It should be noted, however, that the overall resistance to chloride ingress is not wholly dependent on the chloride-binding capacity of a concrete mix. Of at least equal (and possibly more) importance is the nature of the concrete micro structure. For example, even a binder such as silica fume which does not contain significant amounts of aluminium can refine and improve the pore structure, thereby retarding chloride ingress. This would suggest that *multi*-component ***pc*** mixes containing ***sf*** as well as one or more of the high alumina content pozzolanic binders ***mk***, ***pfa*** and ***ggbs*** are likely to provide the highest resistance to chloride ingress. Indeed, this would seem to fit the empirical evidence [31]. However, it is unlikely that any measure can provide indefinite protection, merely delaying the inevitable chloride induced corrosion of the steel reinforcement.

Acknowledgement

We thank the Engineering and Physical Sciences Research Council for financial support (Grants GR/K94874 and GR/M02200).

References

1. R. K. DHIR, M. R. JONES and M. J. McCARTHY, *Proc. Inst. Civ. Engrs.* **99**(2) (1993) 167.
2. (a) P. J. JACKSON, in "Lea's Chemistry of Cement and Concrete," 4th ed., edited by P. C. Hewlett (Arnold, London, 1998) Ch. 2, p. 36; (b) W. CONSHOHOCKEN, PA:ASTM, C 595-M, American Society for Testing and Materials, 1995.
3. (a) P. J. JACKSON, in "Lea's Chemistry of Cement and Concrete," 4th ed., edited by P. C. Hewlett (Arnold, London, 1998) Ch. 2, p. 33; (b) *Idem.*, *ibid.* Ch. 2, p. 35; (c) British Standards Institute, DDENV 197-1, London:BSI, 1995; (d) P. J. JACKSON, in "Lea's Chemistry of Cement and Concrete," 4th ed., edited by P. C. Hewlett (Arnold, London, 1998) Ch. 2, p. 38; (e) M. H. ZHANG and V. M. MALHOTRA, *Cem. Conc. Res.* **25** (1995) 1713.
4. (a) M. R. JONES, R. K. DHIR and B. J. MAGEE, *Cem. Conc. Res.* **27**(6) (1997) 825; (b) R. K. DHIR and M. R. JONES, in Proc. Int. Ash Symp., Lexington, Kentucky, U.S.A., 1997; (c) R. K. DHIR, M. A. K. EL-MOHR and T. D. DYER, *Cem. Conc. Res.* **26**(12) (1996) 1767; (d) R. K. DHIR, M. R. JONES and M. J. McCARTHY, *ibid.* **26**(12) (1996) 1761; (c) G. K. GLASS, N. M. HASSANEIN and N. R. BUENFELD, *Mag. Conc. Res.* **49** (1997) 323.
5. C. A. FYFFE, "Solid State NMR for Chemists" (C. F. C. Press, Guelph, Ontario, Canada, 1983).
6. T. J. BASTOW, J. S. HALL, M. E. SMITH and S. STEUERNAGEL, *Mater. Lett.* **18** (1994) 197.
7. E. KUNDLA, A. SAMOSUN and E. LIPPMAA, *Chem. Phys. Lett.* **83** (1981) 229.
8. J. SKIBSTED, E. HENDERSON and H. J. JAKOBSEN, *Inorg. Chem.* **32** (1993) 1013.
9. A. SAMOSON and E. LIPPMAA, *Phys. Rev. B* **28** (1983) 6567.
10. (a) D. FENZKE, D. FREUDE, T. FRÖLICH and J. HAASE, *Chem. Phys. Lett.* **111** (1984) 171; (b) D. MASSIOT, B. COTE, F. TAULELLE and J. P. COUTURES, in "Applications of NMR Spectroscopy to Cement Science," edited by P. Colombet and A. R. Grimmer (Gordon and Breach Science Publishers, Amsterdam, 1994) Ch. II. 8, p. 157; (c) P. P. MAN, J. KLINOWSKI, G. TROKINER, H. ZANNI and P. PAPON, *Chem. Phys. Lett.* **119** (1985) 143.
11. (a) P. FAUCON, T. CHARPENTIER, D. BERTRANDIE, A. NONAT, J. VIRLET and J. C. PETIT, *Inorg. Chem.* **37** (1998) 3726; (b) P. FAUCON, T. CHARPENTIER, A. NONAT and J. C. PETIT, *J. Am. Chem. Soc.* **120** (1998) 12075.
12. D. FREUDE, J. HAASE, J. KLINOWSKI and T. A. CARPENTER, *Chem. Phys. Lett.* **119** (1985) 365.
13. J. P. AMOUREUX, E. COCHON and L. DELMOTTE, in "Applications of NMR Spectroscopy to Cement Science," edited by P. Colombet and A. R. Grimmer (Gordon and Breach Science Publishers, Amsterdam, 1994) Ch. VI.31, p. 481.
14. D. MÜLLER, A. RETTEL, W. GESSNER, J. P. BAYOUX and A. CAPMAS, *ibid.* Ch. III.18, p. 259.
15. P. J. BARRIE, *Chem. Phys. Lett.* **208** (1993) 486.
16. M. G. MORTUZA, R. DUPREE and S. C. KOHN, *Appl. Magn. Reson.* **4** (1993) 89.
17. A. K. SURYAVANSHI, J. D. SCANTLEBURY and S. B. LYON, *Cem. Conc. Res.* **26** (1996) 717.
18. M. H. ROBERTS, *Magazine Conc. Res.* **14** (1962) 143.
19. J. BARRAS, J. KLINOWSKI and D. W. McCOMB, *J. Chem. Soc., Faraday Trans.* **90** (1994) 3719.
20. F. J. TANG and E. M. GARTNER, *Adv. Cem. Res.* **1** (1988) 67.
21. (a) K. L. SCRIVENER and A. CAPMASS, in "Lea's Chemistry of Cement and Concrete," 4th ed., edited by P. C. Hewlett (Arnold, London, 1998) Ch. 13, p. 723; (b) A. B. KUDRYAVTSEV, T. V. KOUZNETSOVA, W. LINERT and G. HUNTER, *Cem. Concr. Res.* **27** (1997) 501; (c) A. B. KUDRYAVTSEV, T. V. KOUZNETSOVA and A. V. PYATKOVA, *ibid.* **20** (1990) 407.
22. (a) H. F. W. TAYLOR, "Cement Chemistry," 2nd ed. (Thomas Telford, London, 1997) Ch. 6; (b) A. K. SURYAVANSHI, J. D. SCANTLEBURY and S. B. LYON, *Cem. Conc. Res.* **26** (1996) 717.
23. D. DAIMDOT and F. P. GLASSER, *Cem. Conc. Res.* **23** (1993) 221.
24. I. ODLER, in "Lea's Chemistry of Cement and Concrete," 4th ed., edited by P. C. Hewlett (Arnold, London, 1998) Ch. 6, p. 260.
25. M. MORANVILLE-REGOURD, *ibid.* Ch. 11, p. 654.
26. F. MASSAZZA, *ibid.* Ch. 10, p. 518.
27. H. F. W. TAYLOR, "Cement Chemistry," 2nd ed. (Thomas Telford, London, 1997) Ch. 6, p. 173.
28. R. A. HANNA, P. J. BARRIE, C. R. CHEESEMAN, C. D. HILLS, P. M. BUCHLER and R. BERRY, *Cem. Conc. Res.* **25** (1995) 1435.
29. I. G. RICHARDSON, A. R. BROUGH, R. BRYDSON, G. W. GROVES and C. M. DOBSON, *J. Amer. Ceram. Soc.* **76** (1993) 2285.
30. (a) S. GOÑI, C. ANDRADE and C. L. PAGE, *Cem. Conc. Res.* **21** (1991) 635; (b) M. A. SAN JUÁN, *J. Mater. Res.* **32** (1997) 6207.
31. M. R. JONES, R. K. DHIR and B. J. MAGEE, *Cem. Conc. Res.* **27**(5) (1997) 789.

Received 15 September 1999
and accepted 8 March 2000